

Method Article

Development of invasive plant recognition system based on deep learning

ABSTRACT

A major ecological issue that has seriously harmed both human society and the environment is the invasion of alien plants. To stop the invasion of alien plants, it is crucial to create an effective and precise monitoring and early warning system. In this situation, deep learning and computer vision have significant potential to enhance plant monitoring on a wide scale. This study suggests a deep learning-based approach for identifying invasive plants. The user interface is developed as a mobile application (APP). The identification result can be acquired in 1 to 2 seconds after downloading the plant image from the APP, uploading it to the server, and using the convolutional neural network (CNN). The system had an average accuracy of 90.39% on the test set thanks to data augmentation and enhanced networks. The deep learning-based invasive plant identification system created in this study has demonstrated through experiments that it may effectively support botanical research and ecological environment monitoring.

Keywords: alien plant, deep learning, mobile client, CNN, image recognition

1. INTRODUCTION

The ecological problem of alien plant invasion has seriously harmed both human society and the natural world. Alien plant invasion has been linked to numerous studies that demonstrate how it negatively affects the stability, ecosystem function, and species richness of nearby ecosystems. Moreover, the invasion of alien plants will impact the management of water resources, urban forestry [1], and agricultural productivity [2]. In order to safeguard the ecological environment and promote sustainable development, it is crucial to effectively prevent and regulate the invasion of alien plants.

Conventional techniques for identifying alien plants mostly rely on personal professional experience, reference materials, web images for comparison, or obtaining professional identification. Yet, because there are so many different alien plants, there is a lot of variance among the same species of plants despite similarities in appearance. As a result, this artificial identification method for alien plants is ineffective and sensitive to human bias [3].

In the past 20 years, a large number of academics both domestically and internationally have conducted research on the automatic recognition of alien plants based on photographs thanks to the development and use of image processing technology. Initially, high-quality photos of alien plants are acquired using a variety of image acquisition tools. Next, image features are extracted, namely SIFT [4] and HOG [5] in the case of local features and color [6], shape [7], or texture [8] for global features. On a small number of types and sample sets, the traditional pattern recognition techniques mentioned above can produce good recognition results. Several study findings, however, have not been used in actual

39 production because of the model's limited resilience and weak generalization ability, which
40 result from the requirement to manually create features.

41

42 Deep learning techniques have gained increasing attention in recent years for their use in
43 tracking alien plants. The accuracy and effectiveness of identifying alien plants is
44 substantially improved by deep learning techniques like convolutional neural networks (CNN)
45 and recurrent neural networks (RNN), which automatically extract information from collected
46 photos [9,10,11]. When compared to conventional image processing-based techniques,
47 CNNs enable effective analysis of image texture, or the contextual data of numerous nearby
48 pixels. The effective analysis of these textures is made possible by CNNs' self-learning
49 abilities, which can also reveal the vital leaf and canopy characteristics needed to recognize
50 vegetation communities or species [12]. Hence, CNN will fundamentally alter our ability to
51 categorize and identify plants as a result of the development of high-resolution sensor
52 technologies.

53

54 CNN were created with the purpose of classifying images. Software like Flora Incognita or
55 Plannet, which can name a species to plant images, are examples of plant recognition. Such
56 a Network automatically pulls contextual elements from a dataset of photos, learns which of
57 these features (for example, leaf shapes [13] or attributes of the flowers [14]), and then
58 categorizes each image based on observations. The self-learning capability of CNNs is a
59 huge advantage in terms of processing power and automation, as no feature engineering
60 procedure is necessary, given the variety of approaches and scales for representing
61 backgrounds. Several successive pooling procedures that combine feature maps from
62 convolutions to coarser spatial scales, hence boosting the robustness and effectiveness of
63 the network, are a crucial part of a CNN architecture to recognize these features. Only
64 (aggregated) information, i.e., if characteristics indicating the target class are evident
65 everywhere in the image, will be present in the network's final layer. According to CNN, there
66 are few studies on the monitoring of plant invasion in the pertinent literature [15]; instead,
67 studies on plant identification and classification, agricultural pest identification, and plant leaf
68 disease research are more prevalent [16].

69

70 In order to address the issue that farmers or volunteer plant protection workers cannot
71 identify invasive plants in the field, this paper suggests monitoring plant invasion based on
72 CNN and uses deep learning and Android technology to develop a terminal-oriented
73 intelligent identification and monitoring system for plant invasion. In particular, taking images
74 of invasive plants and uploading them to the system's Android mobile terminal can enable
75 automatic identification and give consumers individualized advice on how to control those
76 plants.

77

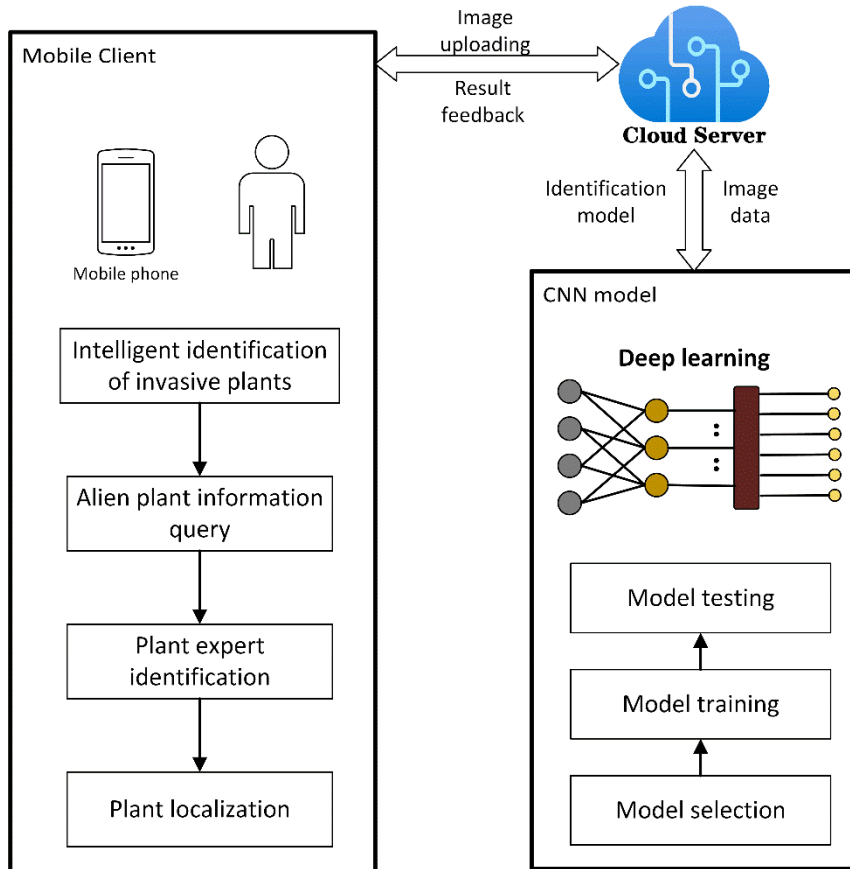
78

79 **2. METHODOLOGY**

80

81 Figure 1 depicts the general layout of the mobile terminal-oriented alien plant invasion
82 monitoring system. An agricultural pest identification model, a cloud server, and a mobile
83 APP make up the system. Images of plants are captured by the mobile APP, which then
84 transmits them over the network to a cloud server. The invasive plants are identified using
85 the identification model placed on the cloud server, and the mobile end receives the results.

86

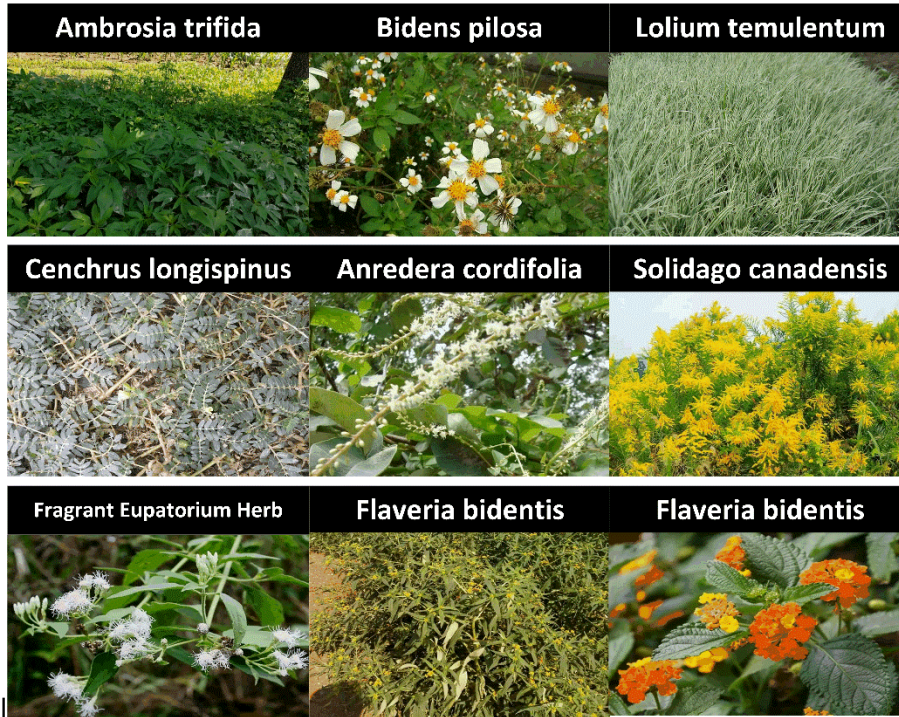


87
88
89
90
91
92
93
94
95
96
97
98
99
100
101
102

Fig. 1. Design of alien plant invasion monitoring system for mobile terminal

2.1 Invasive plant species and data sets

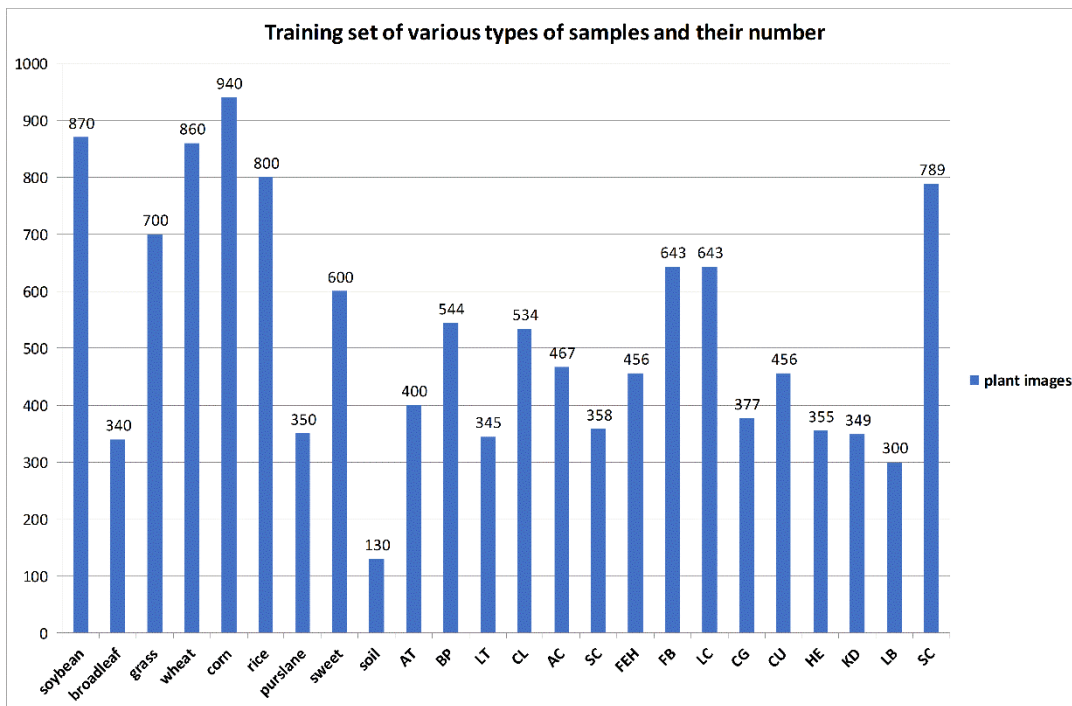
This study's datasets were primarily gathered via the Internet and field photography, which involved simultaneously photographing a variety of plants while collecting open-source image databases and internet-related photographs. According to plant species, all photos were categorized, sorted, and manually marked. In Figure 2, a few pictures of invasive plants are displayed. There are a total of 25 categories in this collection, which includes photos of 9 different common plants and 16 different alien plant kinds. There are 12606 RGB plant picture samples altogether after some unbalanced samples have been extended and enhanced. Also, the collection of invasive plant picture data is divided at random into the training set and the test set, which correspond to an 8:2 ratio.



103
104
105
106
107
108
109
110

Fig. 2. Examples of alien invasive plant images

Use the python program to encode, and view the number of each category in the gathered plant and invasive plant picture data set. Manually name the 25 species in the data set. The breakdown of the training set's sample count for each category is shown in Figure 3.



111

112
113
114
115
116
117
118
119
120
121
122
123
124
125
126
127
128
129
130
131
132
133
134
135
136
137
138
139
140
141
142
143
144
145
146
147
148
149
150
151
152
153
154
155
156
157
158
159
160
161

Fig. 3. Quantity details of samples in each category in training set

2.2 image pre-processing

It is crucial to create an accurate and comprehensive data set because deep learning algorithms often need a lot of data to work well. To train the model for precise monitoring and prediction in the alien plant invasion monitoring system, the dataset should contain photos of various alien plant species in various regions. Nevertheless, the source photos frequently have issues like noise, occlusion, and uneven lighting, which will negatively impact the model's performance during training. In order to enhance image quality and model accuracy before deep learning, the dataset's images must be pre-processed [17].

The image is 256 x 256 pixels in its original size. The scale of the image is evenly changed to 227 X 227 pixels in order to match the input size of the network. A Python script is then used to perform random flipping, random angle rotation, and other data improvement actions on selected imbalanced samples. Also, we must normalize the gamut of pixel intensity values found in the dataset's leaf image before training the CNN network [18]. This step is required because the recovered feature vector from the input image should have all of its dimensions in the same intensity range. This enables the training phase of our CNN model to converge more quickly.

The method of image normalization is to subtract the value $I(i, j)$ of each pixel from the average value μ of the input image, and then divide it by the standard deviation σ of the input image. The distribution of the output pixel intensity value will be similar to a zero-centered Gaussian curve. We use the following formula (1) to normalize each image in the training set:

$$O(i, j) = \frac{I(i, j) - \mu}{\sigma} \quad (1)$$

Information Among them, I and O are the input image and the output image respectively, i, j are the pixel index to be normalized

2.3 Plant classification method based on improved DenseNet model

2.3.1 DenseNet Model

Huang et al. presented the DenseNet convolutional neural network model in 2017 [19]. The network makes use of the ResNet structure to connect the front and back layers, which facilitates gradient back propagation and the training of deeper networks. The DenseNet model can achieve feature reuse, minimize the gradient disappearance issue, simplify the model by using fewer parameters, and increase the propagation and use rates of features. DenseNet is made up of transition layers and a number of dense blocks. Every layer in a dense block takes input from all layers before it, and each layer then generates an output that is connected to all inputs before it and passed to the following layer. The effectiveness of feature propagation is increased by this thick connectivity, which enables each layer to make use of the knowledge from all preceding levels. These two components are then introduced in turn.

More radical than ResNet's connection scheme is DenseBlock, a densely connected block in the DenseNet convolutional neural network architecture. The residual network serves as the foundation for DenseBlock's evolution. Each layer of the residual network is connected to the preceding one or two layers using this connection approach. By adding, or increasing the

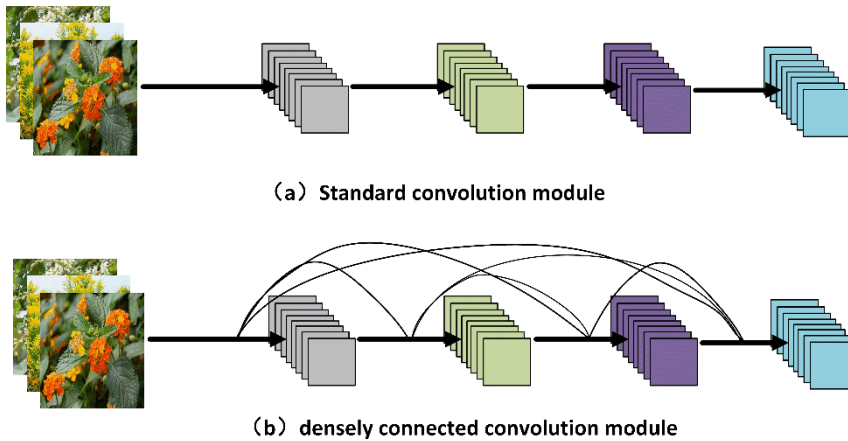
162 input from the preceding layer, the short-circuit connection is created, as shown in formula
 163 (2).
 164

$$165 \quad x_l = H_l(x_{l-1}) + x_{l-1} \quad (2)$$

166
 167 In order to achieve feature reuse, DenseNet uses a dense connection technique to connect
 168 all layers to one another, with each layer being connected to all preceding layers in the
 169 channel dimension, as shown in formula (3).
 170

$$171 \quad x_l = H_l(x_0, x_1, \dots, x_{l-1}) \quad (3)$$

172
 173 x_l is the input of the L layer, which takes the convolution feature $x_0 \sim x_{l-1}$ from all the
 174 preceding layers as input; $(x_0, x_1, \dots, x_{l-1})$ is the splicing operation of the output feature map
 175 from the input layer to the L-1 layer; and $H_l(*)$ is a nonlinear transformation function, which
 176 combines the functions of the BN layer, ReLU layer, and convolution layer. Figure 4 depicts
 177 the architecture of the dense connection module and the common convolution module.
 178
 179



180
 181
 182 **Fig. 4. Structure comparison diagram of standard convolution module and**
 183 **DenseBlock module**

184
 185 In the DenseNet model, the Transition module's function is to compress the model. 1 X 1
 186 convolutional layer is added between the 2 X 2 pooling layers between the dense blocks of
 187 two identical feature maps to minimize the size. The number of channels transferred to the
 188 next dense block is cut in half, and there are fewer parameters, which helps speed up the
 189 network model's convergence when the compression factor in the DenseNet network is set
 190 to 0.5.

191

192

193 **2.3.2 DenseNet-SPP Model**

194

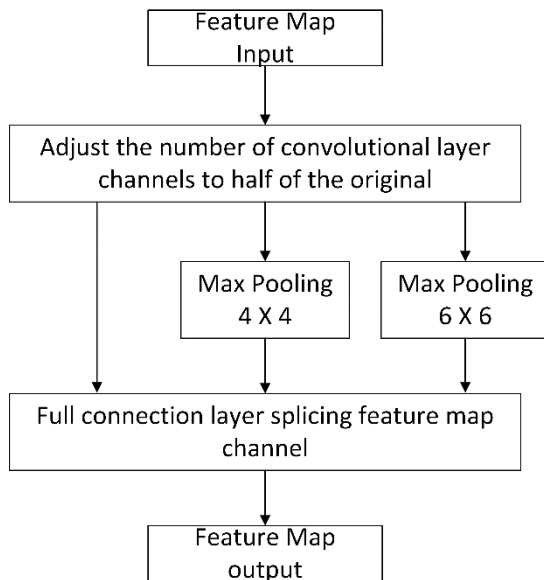
195 He et al. (2015) presented a pyramid pooling SPP (Spatial Pyramid Pooling) [20] structure to
 196 address the issue of input image size limitation in image classification applications. Before to
 197 the completely linked layer, a structure known as the SPP structure is used to create the
 198 network at various scales. To improve the network's ability to recognize objects of various

199 scales, the data are pooled and features from multiple scales are combined. Since there are
200 many different scales and shapes of invasive plants, we believe that adding the SPP
201 structure to the DenseNet network can further enhance the network's performance.

202

203 A multi-layer feature map's channel is adjusted through the convolution of the last layer, and
204 SPP structure is added before the full connection layer and the final convolution layer. Each
205 feature map in this study is separated into several sizes based on 16 X 16, 4 X 4, and 1 X 1.
206 The feature map is converted into a fixed length feature vector through the splicing channel
207 and utilized as the input of the entire connection layer after the grid and Max Pooling
208 operation on each grid. Each feature map is coupled to a 1 X 1 convolution layer to
209 compress and alter the channel dimension. Often, the SPP structure pools via different size
210 windows to obtain feature maps with varied resolutions. In Figure 5, the SPP structure is
211 displayed.

212



213

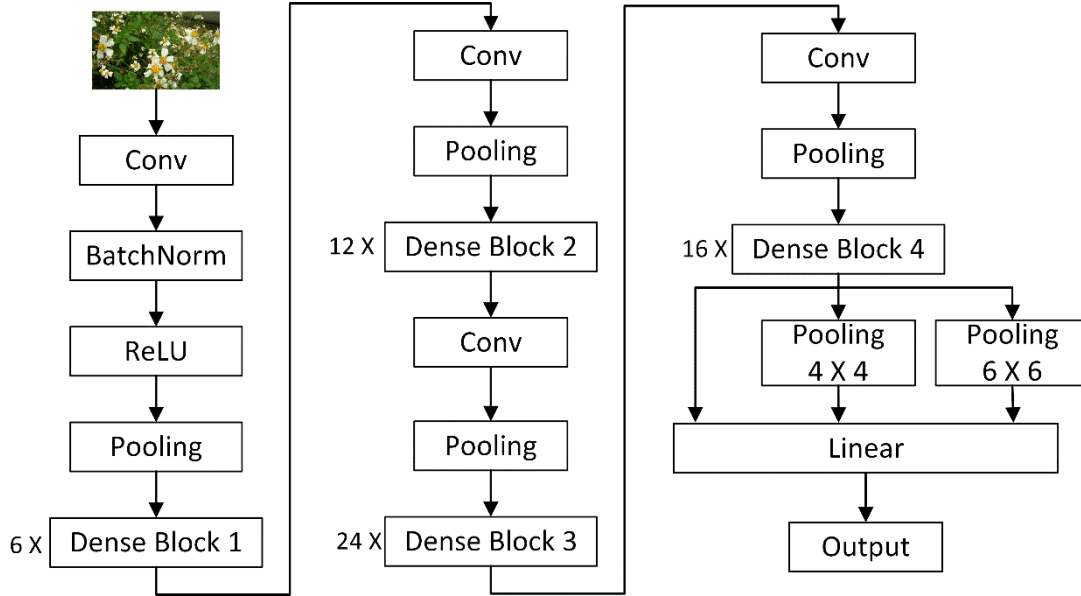
214

215 **Fig. 5. SPP structure diagram illustration**

216

217 An SPP layer is added to the last dense block of DenseNet to pool multi-scale features. The
218 feature map is then input into the fully connected layer for classification jobs, although the
219 fully connected layer needs to be changed based on the data set. The connecting layer's
220 output dimension and category count. The 25 categories used to categorize the invasive
221 plants under study in this paper result in 25 outputs for the completely connected layer. This
222 research specifies the maximum pooling scales of 6 X 6 and 4 X 4 respectively to adapt to
223 the various sizes of invasive plants while taking into account the proportion of invasive plants
224 on the image. In Figure 6, DenseNet's entire network architecture with the SPP structure is
225 displayed.

226



227

228

229

230

231

232

233

234

235

236

237

238

239

240

241

242

243

244

245

246

247

248

249

250

251

252

253

254

255

256

257

Fig. 6. DenseNet network structure diagram with SPP

3. IMPLEMENTATION

The details of the intrusion plant detector's deployment on a cloud server and a mobile terminal are introduced in this part.

3.1 DenseNet-SPP model Implementation

This paper investigates and enhances the image classification network based on the previous research. The network structure $f(\theta)$, loss function L , and learning rate L_R are trained using the invasive plant picture data set $X(x_1, x_2, \dots, x_n)$ and the matching m category $Y(y_1, y_2, \dots, y_m)$. The following describes the algorithm training method.

i) Based on the pre-defined Batch size for normalizing pre-processing, choose training batch $X(x_1, x_2, \dots, x_n)$ from the training set. According to the following Formula (4) computation, the RGB three channels for each image of an invasive plant in the training batch are assigned to the mean value $\mu_{r,g,b} = (0.485, 0.456, 0.406)$ and the standard deviation $\sigma_{r,g,b} = (0.229, 0.226, 0.225)$, respectively.

$$O_r = \frac{I_r - \mu_r}{\sigma_r}; \quad O_g = \frac{I_g - \mu_g}{\sigma_g}; \quad O_b = \frac{I_b - \mu_b}{\sigma_b} \quad (4)$$

In formula (4), I_r , I_g , I_b are the RGB three-channel pixel value of the image before normalization, and O_r , O_g , O_b are the RGB three-channel pixel value of the normalized image

ii) The network receives the normalized training batch $X'_1(x'_a, \dots, x'_b)$ and begins forward propagation to extract features. The feature map acquired by the n th layer in DenseBlock is

258 created by connecting and convolving the feature maps in all levels up to n-1. The
259 computation's formula can be seen in (5)
260

$$261 \quad M_n = F(M_1 \oplus M_2 \oplus \dots \oplus M_{n-1}) \quad (5)$$

262 In Equation (5), M_n represents the output feature of the nth layer of the network, F
263 represents the convolution operation, and \oplus represents the interconnection operation
264 between the features, so it can be obtained that the n-th layer network has $(n^2 + n)/2$
265 connection operations
266

267 iii) Following the network's training of the training batch, the corresponding category Y_1' is
268 determined. The loss L_1 is then determined in accordance with the predicted category Y_1' and
269 the actual category Y_1 , as indicated in formula (6):
270

$$271 \quad \begin{aligned} Y_1' &= f(\theta, X_1') \\ L_1 &= L(Y_1, Y_1') \end{aligned} \quad (6)$$

272 In this paper, the cross-entropy loss function is used in the training process to solve the
273 problem of unbalanced positive and negative samples. The cross-entropy loss function is
274 shown in formula (7):

$$275 \quad L_1 = -\frac{1}{b-a} \sum_{i=1}^{b-a} \sum_{c=1}^m p_{ic} \log(q_{ic}) \quad (7)$$

276 In Equation (7), b-a represents the number of samples in each training batch, c represents
277 the number of categories in total m, and p_{ic} is a symbolic function. If the real category of the
278 ith sample in the training batch is the same as that of category c, it is taken as 1, otherwise
279 0, and q_{ic} represents the probability that the ith sample in the predicted training batch
280 belongs to category c.
281

282

283 iv) The calculated loss L back propagation update network weight Θ , as shown in Formula
284 (8):
285

$$286 \quad \theta' = \theta - L_r \times \nabla g(L_1) \quad (8)$$

287

288 v) The subsequent training batch is chosen to repeat the preceding processes if the traversal
289 is not finished. If the traversal is finished, the training batch satisfaction is assessed and the
290 model weight parameter file for the round is saved.
291

292

293 vi) Repeat the previous stages if the training rounds are not reached; once they are, the
294 model training will be completed.

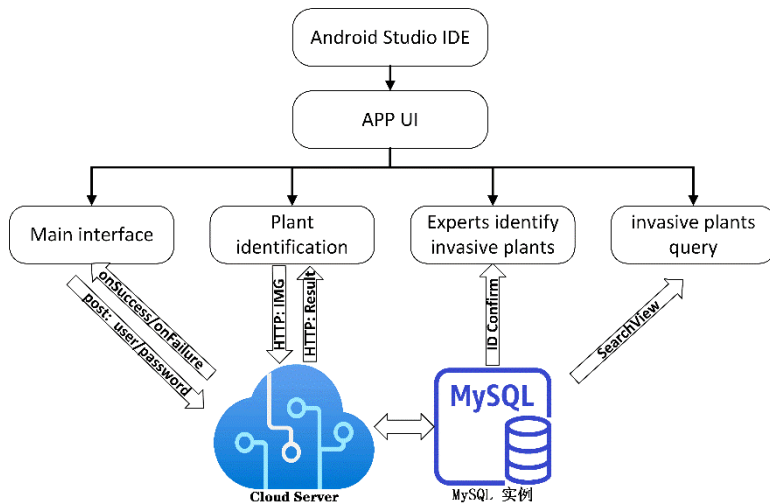
295

295 **3.2 Mobile APP design**

296

297 The Android Integrated Development Environment (Android Studio IDE), which is built on the
298 Windows 10 system platform, is used to create the intrusion plant detector's user interface. It
299 transmits data to the server using the Okhttp network transmission framework and
300 downloads third-party jar development packages, placing them in the lib directory. Following
301 synchronization, it is parsed into a so file before being passed over to the third-party API.
302

303 According to Figure 7, the UI interface of the APP uses a bottom navigation bar. The user
 304 login main interface, the plant intelligent identification module, the invasive plant question
 305 module, and the invasive plant expert identification module are all included in the APP
 306 interface design.
 307



308
 309

310 **Fig. 7. APP design process**

311

312 By sending a post request with information parameters such a user name and password, the
 313 user login module connects to the server. The login success or failure status is displayed
 314 once the server accepts the request and returns callback information
 315 onSuccess()/onFailure()).
 316

317

318 The plant intelligent recognition module offers two image gathering techniques—camera
 319 photography and gallery selection—and communicates with the server and mobile device
 320 using the HTTP protocol. After receiving the image, the server invokes the plant recognition
 321 model to do recognition, and then the client is provided with the recognition result in JSON
 322 data format.

323

324 The invasive plant information query module writes and implements the invasive plant
 325 introduction interface using the SearchView control and the ListView control, and uses the
 326 ViewPager component to switch between various View interfaces. It implements the invasive
 327 plant interface's search functionality using Filter.

328

329 Only users whose identity information is "expert" can identify invasive plants, and the expert
 330 identification module of invasive plants primarily uses the MySQL database. The server will
 331 keep a record of each user's identification so that others can search and find them.

332

333 This paper packages and deploys the program of the agricultural pest recognition model on
 334 the remote server of Alibaba Cloud for the deployment of the server-side recognition model.
 335 It also adds the mean file, weight file, and label file during the model training process, calls
 336 the model, and outputs the recognition. A dll dynamic link library is created once the
 337 software has been compiled. The server calls the invasive plant identification model and
 338 runs the dll dynamic link file when it receives the plant image sent from the mobile terminal in
 339 order to recognize the image that has been uploaded. The submitted photographs and
 340 recognition results are kept in the database while the server feeds back the results to the
 client, making it simple for plant images to be traced in the future.

341
342
343
344
345
346
347
348
349
350
351
352
353
354
355
356
357
358
359

4. EXPERIMENTAL DETAILS

We conduct an experimental evaluation of the DenseNet-SPP model's performance. It is important to note that after 310,000 training cycles on the MS COCO dataset [21], we employ the approach of transfer learning to generate weight files to initialize the DenseNet-SPP network weight in order to prevent data overfitting and produce a more robust model.

4.1 Experiment parameter

The training and testing environments of this experiment are the same, both being Windows 10 operating systems, and the Pytorch deep learning framework is used to realize the training and testing process of the complete model. The specific parameters of the experimental environment are presented in Table 1:

Table 1. Benchmark model comparison experiment environment

Test environment	Deploy
CPU	Inter(R) i7-9700 CPU @3.00GHz
GPU	NVIDIA GeForce 1650 4G
RAM	16G
Python	3.8
Pytorch	1.10.1

360
361
362
363
364
365
366
367
368
369
370

GoogleNet [22], ResNet-50 [23], DenseNet-121 [19], DenseNet-SPP (our), and MobilNet-V2 [24] are the five widely used classical convolutional neural network models chosen for the experiment's benchmark model comparison studies. Following that, the improved model in this work is compared to the performance of these five models. Table 2 displays the comprehensive parameter comparison analysis of these five models. The mAP column's value is the detection performance score that was learned using the MS COCO data set [25].

Table 2. Model performance comparison table

Model	Accuracy (top-1)	Accuracy (top-5)	mAP (COCO)	Parent
GoogleNet	77.9%	93.7%	36.8	23.9M
ResNet-101	74.9%	92.1%	40.8	25.6M
DenseNet-121	75.0%	92.3%	39.8	8.1M
MobilNet-V2	71.3%	90.1%	30.6	3.5M

371
372
373
374

After repeated attempts, the selected training-related hyperparameter values in this experiment are shown in Table 3.

375 **Table 3. Network training hyperparameters**

376

hyperparameters	Accuracy (top-1)
Num Class	8
Optimizer	Adam
Learning rate	0.0001
epochs	200

377

378

379 4.2 Evaluating indicator

380

381 Several evaluation indices in the MS COCO data set are frequently utilized in target
 382 detection algorithm research to assess the benefits and drawbacks of the algorithm. The
 383 most crucial metric is Average Precision (AP), which shows how well a certain kind of target
 384 can be detected. Intersection-over Union (IoU), which symbolizes the overlapping of two
 385 instance masks, defines AP. There are some additional significant performance metrics, but
 386 since the accuracy of target identification is the main concern of this work, other indicators
 387 are not contrasted in it. Calculations for AP and mAP are displayed in (9) ~ (12). In order to
 388 avoid affecting the accuracy and recall rate, the assessment index mAP (IoU = 0.50:0.05:
 389 0.95) was chosen.

390

$$391 \quad P = \frac{TP}{TP + FP} \quad (9)$$

$$392 \quad R = \frac{TP}{TP + FN} \quad (10)$$

$$393 \quad AP = \int_0^1 P(R) dR \quad (11)$$

$$394 \quad mAP = \frac{mAP_{0.50} + mAP_{0.55} + \dots + mAP_{0.95}}{10} \quad (12)$$

395

396 Among them, TP denotes the proportion of samples for which the model's predicted
 397 category matches the actual label category; FP, the proportion of samples for which the
 398 model's predicted category does not match the actual label category; and FN, the proportion
 399 of samples for which the predicted category was background but the actual label was
 400 something else.

401

402

403 5. RESULTS AND DISCUSSION

404

405 We experimentally evaluated our prototype implementation regarding classification accuracy
 406 and performance. We installed instrumentation in the mobile app running on a smartphone
 407 to measure the preprocessing, and invasive plant recognition processes.

408

409 5.1 Model performance

410

411

412 In order to verify the performance of our proposed invasive plant detection model DenseNet-
 413 SPP, we trained these five network models for 200 epochs, and the test accuracy is shown
 414 in Table 4:

415
 416
 417
 418

Table 4. Convolutional Neural Network Model Recognition Performance Comparison Table

Model	AT plant		BP plant		LT plant	
	pre	rec	pre	rec	pre	Rec
GoogleNet	0.423	0.632	0.445	0.453	0.628	0.639
ResNet-101	0.614	0.591	0.615	0.632	0.569	0.689
DenseNet-121	0.853	0.923	0.912	0.935	0.806	0.824
MobilNet-V2	0.837	0.844	0.850	0.726	0.740	0.715
Our	0.872	0.941	0.926	0.881	0.811	0.815

419

Model	CL plant		AC plant		SC plant	
	pre	rec	pre	rec	pre	Rec
GoogleNet	0.639	0.628	0.776	0.809	0.738	0.776
ResNet-101	0.689	0.569	0.883	0.864	0.861	0.832
DenseNet-121	0.815	0.740	0.811	0.832	0.922	0.911
MobilNet-V2	0.689	0.713	0.753	0.842	0.762	0.755
Our	0.824	0.951	0.915	0.895	0.956	0.953

420

Model	CG plant		KD plant		other plant	
	pre	rec	Pre	Rec	Pre	Rec
GoogleNet	0.749	0.853	0.829	0.875	0.624	0.618
ResNet-101	0.831	0.824	0.851	0.885	0.639	0.688
DenseNet-121	0.869	0.789	0.907	0.886	0.831	0.811
MobilNet-V2	0.758	0.779	0.828	0.879	0.762	0.759
Our	0.889	0.878	0.929	0.912	0.864	0.786

421

422 Table 4 shows that the DenseNet-SPP invasive plant image classification model
 423 outperformed other convolutional neural network models in terms of precision rate and recall
 424 rate on eight different invasive plant species. This indicates that the DenseNet-The SPP
 425 model is better suited for invasive plant image classification tasks than other convolutional
 426 neural network models. Our model has the lowest accuracy rate for LT plant species while
 427 having the best recognition rate for SC plant species, even reaching 95.6% detection
 428 accuracy. Yet, the average identification accuracy of each category is not less than 80%,
 429 demonstrating that the DenseNet-based plant recognizer has a significant impact on the
 430 data set's noise and plant images with occlusion and other comparable traits. robustness.
 431

432 In the data set containing invasive plants, the enhanced algorithm is contrasted with other
 433 algorithms to confirm its superiority and efficacy. The test results are shown in Table 5. This
 434 further demonstrates the efficacy of the approach suggested in this study as the accuracy
 435 rate attained on the above is far greater than that of previous benchmark convolutional
 436 neural network techniques and the upgraded DenseNet algorithm.

437
 438
 439
 440

Table 5. Comparison of the average detection accuracy achieved by the algorithm

Model	mAP (%)
GoogleNet	71.02
ResNet-101	83.22
DenseNet-121	86.29
MobilNet-V2	79.63
Our	90.39

441
 442
 443
 444
 445
 446
 447
 448
 449
 450

5.2 Mobile terminal APP test

An Android-powered phone can have the mobile terminal APP loaded on it. Including the main user login interface, the plant intelligent identification module, the invasive plant query module, and the invasive plant expert identification module, Figure 8 depicts a screenshot of the mobile terminal's APP interface.



451
 452
 453
 454
 455
 456
 457
 458
 459
 460
 461

Fig. 8. APP interface of invasive plants identification based on Android mobile phone

The main user interface Figure 8-(a) is displayed when the user launches the APP for the invasive plant identification system. Ordinary users and experts can register separately on the registration interface. The user must upload a professional credential while registering as an expert, and the intrusion can only be performed after the background check. Plant identification: After a successful registration is made in the system, the plant identification module Figure 8-(b) is immediately connected. The user can upload images or take pictures using this interface and upload them to the server, where the DenseNet-SPP model will

462 identify the images and return the results. Figure 8-(d) is the invasive plant query module,
463 and the user can learn knowledge on this interface. You can also use keyword search to find
464 the details of the invasive plants you want to know. If the user comes across a plant that
465 cannot be identified by the model, he can apply for expert identification. The expert will
466 feedback the identification result on the identification interface, and display Figure 8-(c) on
467 the common user interface. Also, upon testing, the server will utilize the pest identification
468 model and return the results when a user submits it an image of a pest to be recognized.
469 The users' real-time needs can be satisfied in 1 to 2 seconds.

470

471 **6. CONCLUSION AND FUTURE WORK**

472

473 We created a terminal-oriented invasive plant recognition system based on deep learning
474 technology through the experiment and analysis of this study. To increase the model's
475 robustness and accuracy, the system utilizes the DenseNet network topology and
476 preprocesses and enriches the data set. To prevent over-fitting and achieve a greater
477 recognition accuracy, we apply the proper hyperparameter settings and data improvement
478 techniques during the training phase. The system's average accuracy on the test set was
479 90.39%. The system also has a main user login interface, invasive plant question and expert
480 identification modules, and a plant intelligent recognition module. Users can use the APP to
481 snap pictures of unknown invasive plants, upload them to the server for plant recognition,
482 and instantly receive the results of that recognition.

483

484 **ACKNOWLEDGEMENTS**

485

486 A brief acknowledgement section may be given after the conclusion section just before the
487 references. The acknowledgments of people who provided assistance in manuscript
488 preparation, funding for research, etc. should be listed in this section. All sources of funding
489 should be declared as an acknowledgement. Authors should declare the role of funding
490 agency, if any, in the study design, collection, analysis and interpretation of data; in the
491 writing of the manuscript. If the study sponsors had no such involvement, the authors should
492 so state. Also, we will talk about some potential future research in this chapter.

493

494 i) Dataset Expansion. Presently, the majority of datasets have narrow geographic and
495 conceptual coverage, which may restrict the system's ability to generalize to new
496 environments and species. Future research could concentrate on enlarging the existing
497 datasets by include more species and photographs from various places to overcome this
498 problem.

499

500 ii) Model Optimization. Deep learning models are highly complex and can require significant
501 computational resources to train and optimize. As such, future work could focus on
502 developing more efficient models that require less training time and computational
503 resources.

504

505 iii) Integration with Other Technologies. Invasive plant recognition systems can benefit from
506 integration with other technologies, such as unmanned aerial vehicles (UAVs) or ground-
507 based sensors. For example, UAVs can be used to collect high-resolution images of invasive
508 plants from different angles and heights, which can improve the system's ability to recognize
509 plants. Similarly, ground-based sensors can be used to collect environmental data, such as
510 temperature and humidity, which can be used to improve the system's ability to recognize
511 plants under different conditions.

512

513

514 **COMPETING INTERESTS**

515

516 Authors have declared that no competing interests exist.

517

518 **AUTHORS' CONTRIBUTIONS**

519

520 Zhuolei Yang designed the study, performed the statistical analysis, wrote the protocol, and
521 wrote the first draft of the manuscript. Zheming Fan and Chenyu Niu managed the analyses
522 of the study. Peixin Li managed the literature searches. All authors read and approved the
523 final manuscript. **Thank you very much to Ms. Yang Xiaohui for helping us in the process of**
524 **completing the thesis**

525

526

527

528

529 **REFERENCES**

530

531

532 1. Saleem M H, Potgieter J, Arif K M. Automation in agriculture by machine and deep
533 learning techniques: A review of recent developments[J]. Precision Agriculture, 2021, 22:
534 2053-2091. DOI: 10.1007/s11119-021-09806-x

535 2. Kattenborn, T.; Eichel, J.; Fassnacht, F.E. Convolutional Neural Networks enable efficient,
536 accurate and fine-grained segmentation of plant species and communities from high-
537 resolution UAV imagery. Scientific reports 2019, 9, 17656.

538 DOI: 10.1038/S41598-019-53797-9

539 3. Fathi Kazerouni M, Mohammed Saeed N T, Kuhnert K-D. Fully-automatic natural plant
540 recognition system using deep neural network for dynamic outdoor environments[J]. SN
541 Applied Sciences, 2019, 1: 1-18.

542 DOI: 10.1007/s42452-019-0785-9

543 4. Wen, C.; Guyer, D.E.; Li, W. Local feature-based identification and classification for
544 orchard insects. Biosystems engineering 2009, 104, 299-307.

545 DOI: 10.1016/j.biosystemseng.2009.07.002

546 5. Wen, C.; Guyer, D. Image-based orchard insect automated identification and classification
547 method. Computers electronics in agriculture 2012, 89, 110-115.

548 DOI: 10.1016/j.compag.2012.08.008

549 6. Tan, W.; Zhao, C.; Wu, H. Intelligent alerting for fruit-melon lesion image based on
550 momentum deep learning. Multimedia Tools Applications 2016, 75, 16741-16761.

551 DOI: 10.1007/s11042-015-2940-7

552 7. Lowe, D.G. Distinctive Image Features from Scale-Invariant Keypoints. International
553 Journal of Computer Vision 2004, 60, 91-110.

554 DOI: 10.1023/B%3AVISI.0000029664.99615.94

555 8. Dalal, N. Histograms of oriented gradients for human detection. Proc of Cvpr 2005.

556 DOI: 10.1109/CVPR.2005.177

557 9. Kattenborn, T.; Leitloff, J.; Schiefer, F.; Hinz, S. Review on Convolutional Neural Networks
558 (CNN) in vegetation remote sensing. ISPRS journal of photogrammetry remote sensing
559 2021, 173, 24-49.

560 DOI: 10.1016/j.isprsjprs.2020.12.010

561 10. Bah M D, Hafiane A, Canals R. Deep Learning with Unsupervised Data Labeling for
562 Weed Detection in Line Crops in UAV Images[J]. Remote Sensing, 2018, 10(11).

563 DOI: 10.3390/rs10111690

564 11. Azdc A, Hehf A, Jaf B. Computer vision based detection of external defects on tomatoes
565 using deep learning - ScienceDirect[J]. Biosystems Engineering, 2020, 190: 131-144.

566 DOI: 10.1016/j.biosystemseng.2019.12.003

567 12. Ray, P.P. Internet of things for smart agriculture: Technologies, practices and future
568 direction. *Journal of Ambient Intelligence Smart Environments* 2017, 9, 395-420.
569 DOI: 10.3233/AIS-170440

570 13. Alessandro D S F, Matte Freitas D, Gercina G a D S, et al. Weed detection in soybean
571 crops using ConvNets[J]. *Computers Electronics in Agriculture*, 2017, 143: 314-324.
572 DOI: 10.1016/j.compag.2017.10.027

573 14. Jia W, Mou S, Wang J, et al. Fruit recognition based on pulse coupled neural network
574 and genetic Elman algorithm application in apple harvesting robot[J]. *International Journal of*
575 *Advanced Robotic Systems*, 2020, 17(1).
576 DOI: 10.1177/1729881419897473

577 15. Bah, M.D.; Hafiane, A.; Canals, R. Deep learning with unsupervised data labeling for
578 weed detection in line crops in UAV images. *Remote Sensing in Ecology Conservation* 2018,
579 10, 1690.
580 DOI: 10.3390/rs10111690

581 16. Bouguettaya A, Zarzour H, Kechida A, et al. Deep learning techniques to classify
582 agricultural crops through UAV imagery: A review[J]. *Neural Computing Applications*, 2022,
583 34(12): 9511-9536.
584 DOI: 10.1007/s00521-022-07104-9

585 17. Guo S, Wang S, Yang Z, et al. A Review of Deep Learning-Based Visual Multi-Object
586 Tracking Algorithms for Autonomous Driving[J]. *Applied Sciences*, 2022, 12(21): 10741.
587 DOI: <https://doi.org/10.3390/app122110741>

588 18. Chen Y, Tang X, Qi X, et al. Learning graph normalization for graph neural networks[J].
589 *Neurocomputing*, 2022(Jul.7): 493.
590 DOI: 10.48550/arXiv.2009.11746

591 19. Huang, G.; Liu, Z.; Van Der Maaten, L.; Weinberger, K.Q. Densely connected
592 convolutional networks. In *Proceedings of the Proceedings of the IEEE conference on*
593 *computer vision and pattern recognition*, 2017; pp. 4700-4708.
594 DOI: 10.1109/CVPR.2017.243

595 20. He, K.; Zhang, X.; Ren, S.; Sun, J. Spatial Pyramid Pooling in Deep Convolutional
596 Networks for Visual Recognition. *IEEE Transactions on Pattern Analysis & Machine*
597 *Intelligence* 2014, 37, 1904-1916.
598 DOI: 10.1109/TPAMI.2015.2389824

599 21. Lin, T.-Y.; Maire, M.; Belongie, S.; Hays, J.; Perona, P.; Ramanan, D. et al. Microsoft
600 coco: Common objects in context. In *Proceedings of the Computer Vision–ECCV 2014: 13th*
601 *European Conference, Zurich, Switzerland, September 6-12, 2014, Proceedings, Part V 13,*
602 *2014; pp. 740-755.*
603 DOI: https://doi.org/10.1007/978-3-319-10602-1_48

604 22. Szegedy C, Liu W, Jia Y, et al. Going deeper with convolutions[C]. *Proceedings of the*
605 *IEEE conference on computer vision and pattern recognition*, 2015: 1-9.
606 DOI: 10.1109/CVPR.2015.7298594

607 23. He K, Zhang X, Ren S, et al. Deep residual learning for image recognition[C].
608 *Proceedings of the IEEE conference on computer vision and pattern recognition*, 2016: 770-
609 778.
610 DOI: 10.1109/CVPR.2016.90

611 24. Sandler M, Howard A, Zhu M, et al. MobileNetV2: Inverted Residuals and Linear
612 Bottlenecks[J]. *IEEE*, 2018.
613 DOI: 10.1109/CVPR.2018.00474

614 25. Elharrouss, O.; Akbari, Y.; Almaadeed, N.; Al-Maadeed, S. Backbones-Review: Feature
615 Extraction Networks for Deep Learning and Deep Reinforcement Learning Approaches.
616 arXiv preprint arXiv:2206.08016 2022.
617 DOI: <https://doi.org/10.48550/arXiv.2206.08016>
618
619

